IN VITRO RECEPTOR AUTORADIOGRAPHY

Fig. 1

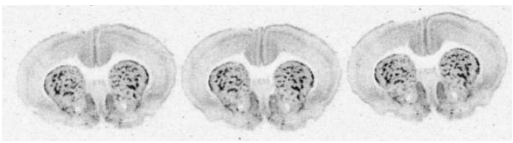

Binding of [^{3}H]DAMGO to μ opioid in coronal sections at the level of the corpus striatum in a rat brain.

Fig. 2

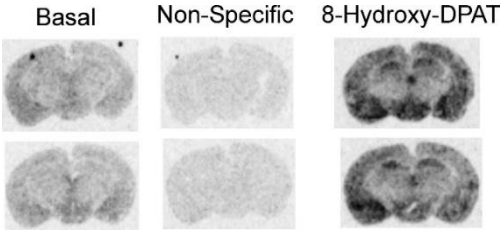

[^{35}S]GTPγS binding in rat brain slices. In the presence of the 5-HT1a agonist, 8-hydroxy-DPAT (10 μM), [^{35}S]GTPγS binding was increased relative to basal levels in the hippocampus, ventral cortex and hypothalamus, reflecting the distribution of agonist-activated receptors. Non-specific [^{35}S]GTPγS binding was defined using unlabeled GTPγS (10 μM).

Fig. 3

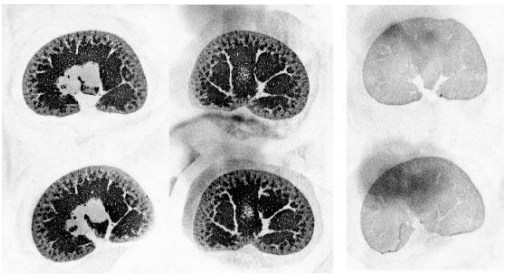

Binding of [^{3}H]LRRK2-IN-1 to the LRRK2 enzyme in rat kidney. Sections on the left are total binding and the two sections on the right non-specific binding, defined using unlabeled LRRK2-IN-1 (10 μM).

Fig. 4

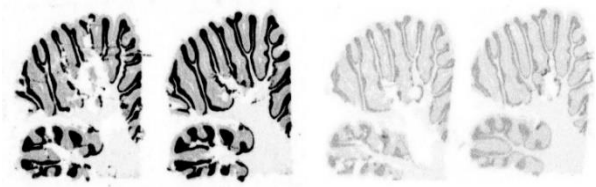

Binding of [^{35}S]TBPS to $GABA_a$ receptors in the dog cerebellum. The two sections on the left are total binding and the two sections on the right non-specific binding, defined using picrotoxin (30 μM)

Fig. 5

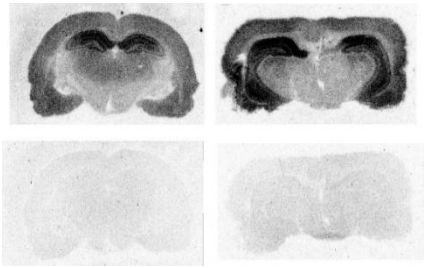

[^{3}H]MK801 binding to NMDA receptors in coronal sections in the rat brain. Upper two sections are total binding and lower two sections non-specific binding, defined using unlabeled MK801 (10 µM).

EX VIVO RECEPTOR AUTORADIOGRAPHY

Fig. 6

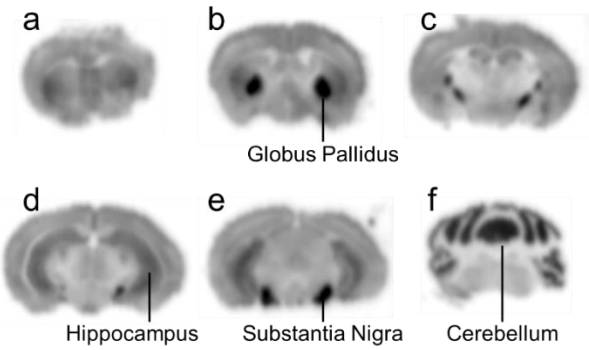

Autoradiography in brain from a mouse administered the radioiodinated cannabinoid CB1 receptor radioligand, [^{125}I]AM2233. Sections (coronal) imaged using phosphor imaging. Radioactivity distribution is consistent with selective binding to the CB1 receptor.